



Kinetic signatures during a quasi-continuous lobe reconnection event: Cluster Ion Spectrometer (CIS) observations

M. B. Bavassano Cattaneo,¹ M. F. Marcucci,¹ A. Retinò,² G. Pallocchia,¹ H. Rème,³ I. Dandouras,³ L. M. Kistler,⁴ B. Klecker,⁵ C. W. Carlson,⁶ A. Korth,⁷ M. McCarthy,⁸ R. Lundin,⁹ and A. Balogh¹⁰

Received 20 January 2006; revised 27 April 2006; accepted 1 June 2006; published 20 September 2006.

[1] On 3 December 2001 the Cluster spacecraft observed a long-lasting lobe reconnection event in the southern high-latitude dusk magnetopause (MP) tailward of the cusp, during a 4 hour interval of mainly northward interplanetary magnetic field (IMF) and of sub-Alfvénic magnetosheath flow. Almost all the MP encounters have accelerated flows (for which the Walén test has been successfully verified by Retinò et al. (2005)) as well as a large number of secondary populations related to reconnection, that is, ions of magnetosheath or magnetospheric origin which cross the MP either way. The detailed analysis of the distribution functions shows that the reconnection site frequently moves relative to the spacecraft, but simultaneous measurements by two spacecraft on opposite sides of the reconnection site indicate that the spacecraft's distance from the X line is small, i.e., below 3200 km. The vicinity to the X line throughout the event is probably the reason why the distribution functions characteristics agree with theoretical expectations on both sides of the reconnection site throughout this long event. Moreover, the detailed analysis of the distribution functions shows evidence, during a few time intervals, of dual reconnection, i.e., of reconnection simultaneously going on also in the northern hemisphere.

Citation: Bavassano Cattaneo, M. B., et al. (2006), Kinetic signatures during a quasi-continuous lobe reconnection event: Cluster Ion Spectrometer (CIS) observations, *J. Geophys. Res.*, *111*, A09212, doi:10.1029/2006JA011623.

1. Introduction

[2] Magnetic reconnection at the magnetopause (MP) is known to be an extremely efficient process to transfer mass, energy and momentum from the solar wind to the magnetosphere. For northward interplanetary magnetic field (IMF) reconnection occurs at high latitude, tailward of the cusp (the so-called “lobe reconnection”), and produces open field lines which unbend sunward and equatorward and field lines which convect tailward. There have been a

number of observations of lobe reconnection, which include also the kinetic aspects: *Gosling et al.* [1991, 1996] observe lobe reconnection on the flanks of the MP and discuss kinetic signatures as well as field line convection. Other studies are those by *Onsager et al.* [2001], *Fuselier et al.* [1995, 1997], *Kessel et al.* [1996], *Avanov et al.* [2001], *Safrankova et al.* [1998], *Phan et al.* [2003], and *Retinò et al.* [2005]. Crucial questions regarding the reconnection process, both equatorward and tailward of the cusp, concern its duration and its large-scale configuration. Long lasting reconnection events have been observed both at low [*Gosling et al.*, 1982; *Phan et al.*, 2000; *Marcucci et al.*, 2000] and at high latitude [*Phan et al.*, 2003, 2004; *Retinò et al.*, 2005].

[3] In order for reconnection to be steady the two magnetic flux tubes resulting from reconnection must contract in opposite directions in an inertial frame, and this occurs only if the magnetosheath flow near the X line is sub-Alfvénic [*Gosling et al.*, 1991]. This is a stringent condition for reconnection on the flanks of the MP or at high latitude. Besides the fluid signatures of reconnection, that is tangential stress balance across the MP, there are a number of characteristic kinetic signatures in the distribution functions of particles streaming along reconnected field lines, that is particles of magnetosheath/magnetospheric origin which are reflected at the MP or transmitted across it. These signatures have been predicted by kinematic

¹Istituto di Fisica dello Spazio Interplanetario, Istituto Nazionale di Astrofisica, Rome, Italy.

²Swedish Institute of Space Physics, Uppsala, Sweden.

³Centre d'Etude Spatiale des Rayonnements, Toulouse, France.

⁴Space Science Center, Center for Earth, Oceans and Space, University of New Hampshire, Durham, New Hampshire, USA.

⁵Max-Planck-Institut für Extraterrestrische Physik, Garching, Germany.

⁶Space Sciences Laboratory, University of California, Berkeley, California, USA.

⁷Max-Planck-Institut für Sonnensystemforschung, Katlenburg-Lindau, Germany.

⁸Geophysics Program, University of Washington, Seattle, Washington, USA.

⁹Swedish Institute of Space Physics, Kiruna, Sweden.

¹⁰Space and Atmospheric Physics, Blackett Laboratory, Imperial College, London, UK.

considerations [Cowley, 1982, 1995] and have later been confirmed by observations [Fuselier, 1995, and references therein]. The interest of the kinetic aspect lies in the fact that it allows the inference of important information on the reconnection topology. The present study concerns the kinetic signatures of reconnection observed during a quasi-continuous lobe reconnection event. The Cluster spacecraft are skimming the high-latitude dusk magnetopause tailward of the cusp in the southern hemisphere during a period of mainly northward IMF and have multiple encounters with the MP during which they detect signatures of reconnection for about four hours. The detailed study of the reconnection event from the fluid point of view, with the Walen test for the accelerated flows, has been described by Retinò *et al.* [2005]. The spacecraft orbits are such that at least one of the Cluster spacecraft is often close to the current sheet, and this allows it to have excellent coverage of the magnetopause for four hours and suggests that reconnection is going on quasi-continuously. The reconnection signatures consist of accelerated tailward flows or sunward flows, depending on whether the spacecraft are located tailward or sunward of the reconnection site, respectively. Moreover, the detection of a few reconnection flow reversals, that is of reconnection flows directed in opposite directions within short time intervals, suggests that at least in a few cases, the spacecraft are close to the reconnection site. A consequence of this favorable configuration is that a large number of secondary populations related to reconnection are detected within the current sheet: these populations are the object of the present study. The structure of the paper is the following: section 2 provides an overview of the event, section 3 discusses kinetic signatures in the current sheet and provides an estimate of the distance from the X line, section 4 concerns the magnetic field line convection following reconnection, section 5 presents one particular MP crossing which has important implications on the overall topology of reconnection, section 6 discusses the global aspects of reconnection, and, finally, section 7 summarizes the main results.

2. Data Set, Orbit, and Event Overview

[4] The event under study occurred on 3 December 2001 between 0730 and 1200 UT. The data used are from the Cluster Ion Spectrometer (CIS) onboard Cluster spacecraft SC1, SC3 and SC4. No CIS data were available on SC2. The CIS experiment consists of two instruments: CODIF, which provides the three-dimensional distribution functions in the energy range of 20 to 40000 eV for four ion species: H^+ , He^+ , He^{++} , and O^+ , and HIA, which provides the three-dimensional distribution functions in the energy range of 5 to 32000 eV, with no mass separation. For the present study, moments and three-dimensional ion distribution functions by CODIF and HIA have been used. Ion data are available with the maximum time resolution, i.e., 4 s, which allows to follow the changes of the distribution functions on short timescales. Spin averaged magnetic field data from the FGM experiment onboard the three spacecraft have also been used. The CIS and FGM experiments have been described by Rème *et al.* [2001] and by Balogh *et al.* [2001], respectively. The Cluster spacecraft are located tailward of the cusp on the dusk flank of the MP, and their orbit during the period of interest lies in the $Y_{GSM}-Z_{GSM}$

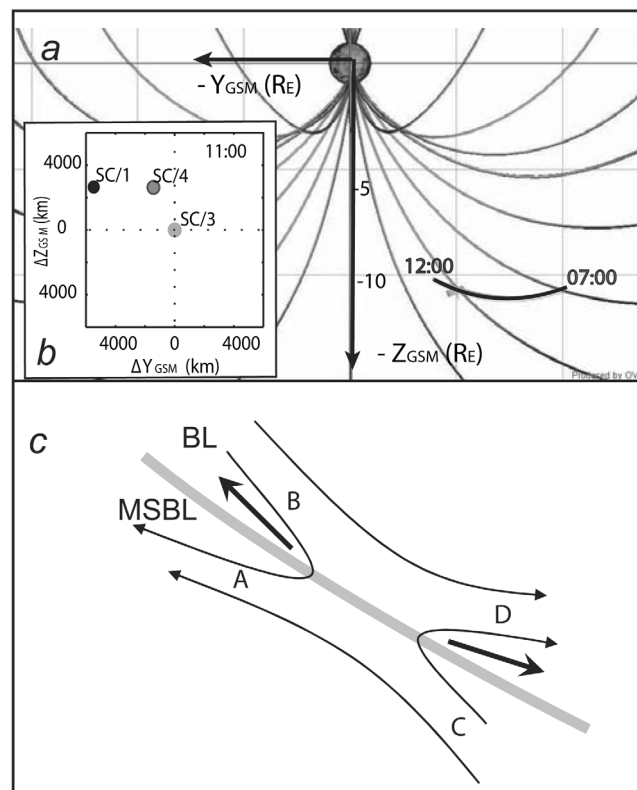


Figure 1. (a) Cluster's orbit in the $Y_{GSM}-Z_{GSM}$ plane (created by Orbit Visualization Tool, <http://ovt.irfu.se>). (b) Position of SC1 and SC4 with respect to SC3 in the $Y_{GSM}-Z_{GSM}$ plane. (c) Sketch of the reconnection topology (adapted from Retinò *et al.* [2005]).

plane and is shown in Figure 1 together with the position of the three spacecraft on the same plane. The spacecraft are skimming the southern high-latitude magnetopause from 17 to 15 GSM local time: SC1 and SC4 are, for most of the time, on the magnetospheric side of the MP, and SC3 is on the magnetosheath side. The separation between the spacecraft is a few thousand kilometers, predominantly on the $Y_{GSM}-Z_{GSM}$ plane, and is smaller along the X_{GSM} axis. An overview of the event is shown in Figure 2: initially, all three spacecraft are in the magnetosheath. At around 0740 UT SC1 and SC4 have an inbound MP crossing followed by a large number of partial crossings throughout the event and spend the rest of the time in the magnetosphere (in the plasma mantle or in the lobes), apart from the interval 1029 to 1037 UT when they briefly sample the magnetosheath. SC3 has a somewhat different story: it has a first complete inbound MP crossing at around 0940 UT, followed by a large number of inbound/outbound MP crossings, until its final entry in the magnetosphere at around 1140 UT. SC3's passages in the magnetosphere usually occur in the lobes, where no significant resident population is present. Note that all three spacecraft are always close to the MP as indicated by their frequent partial and/or complete MP crossings. The magnetosheath magnetic field, except for a few brief intervals, is predominantly northward and sunward ($B_X > 0$ and $B_Z > 0$), and its B_Y component is mainly positive before 0950 UT and negative after that time.

December 3, 2001

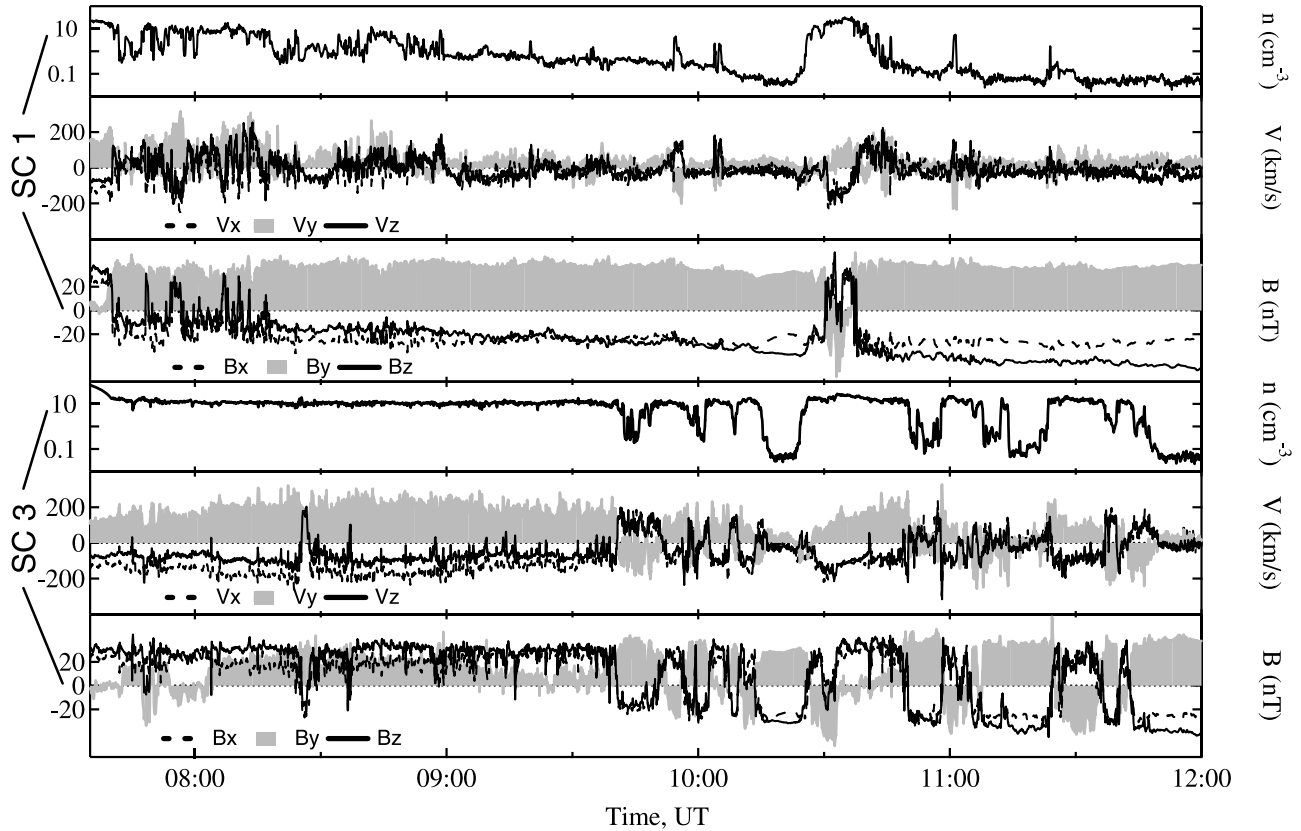


Figure 2. Event overview, from top to bottom n (in cm^{-3}), V (in km/s), B (in nT) for SC1 (above), and SC3 (below). The x component is dashed, and the y component is shaded. SC4 (not shown) is similar to SC1 and differs from it only on small scale. \mathbf{B} and \mathbf{V} are in GSM coordinates.

Therefore, taking into account the magnetospheric field's direction, the shear of the MP crossings is high in the latter part of the event, and somewhat lower in the earlier part. *Retinò et al.* [2005, Figures 6 and 8] show that accelerated flows which satisfy the Walén test are observed at almost all the BL encounters. As these authors point out, one important reason for the long duration of this reconnection event is that the Alfvén Mach number, M_A , in the magnetosheath is usually well below 1, and only occasionally it is close to 1: the reason for the large V_A is probably the relatively high IMF magnitude (10–11 nT at ACE). A sketch of the reconnection topology, as derived by *Retinò et al.* [2005], is shown in Figure 1c. The plane of Figure 1c is roughly the $Y_{GSM} Z_{GSM}$ plane, but the downward side is tilted sunward (and the duskward side is tilted tailward), so that reconnection flows stream sunward-dawnward-northward in one case and tailward-duskward-southward in the other case.

3. Kinetic Signatures in the Current Sheet and Distance From the X Line

[5] When reconnection occurs, a typical MP inbound crossing consists of a magnetic field rotation from the magnetosheath to the magnetospheric orientation followed by a region, the boundary layer (BL), where the plasma density and the field magnitude are intermediate between

the magnetosheath and magnetospheric level. The magnetopause is the region where most of the field rotation occurs and the outer part of the field rotation is the magnetosheath boundary layer (MSBL). In most crossings of 3 December 2001, the regions of field reversal and the BL are usually well defined and clearly separated. A few distribution functions, representative of those observed in the MSBL and in the BL, are presented in Figures 3 and 4. Figures 3a and 3b show two simultaneous distribution functions: SC3 observes an anisotropic (with $T_{\perp} > T_{\parallel}$) typical magnetosheath distribution function, and SC1, in the MSBL, detects two populations: the incident magnetosheath, considerably heated as compared to the simultaneous observation by SC3 and a secondary population which flows along the convected magnetic field direction. The latter population is displaced, with respect to the incident population, by $2V_A$ along the convected magnetic field direction ($V_A = 220 \text{ km/s}$), as predicted for magnetosheath ions reflected off the MP within the current layer [*Fuselier, 1995*]. The fact that the reflected ions stream parallel to the MSBL field means that the spacecraft is located sunward of the reconnection site, i.e., on side A of the sketch of Figure 1c. A similar case of MSBL sunward of the reconnection site is shown in Figure 3c, the only difference being that now the magnetosheath flow is exactly antiparallel to \mathbf{B} with no perpendicular component. In

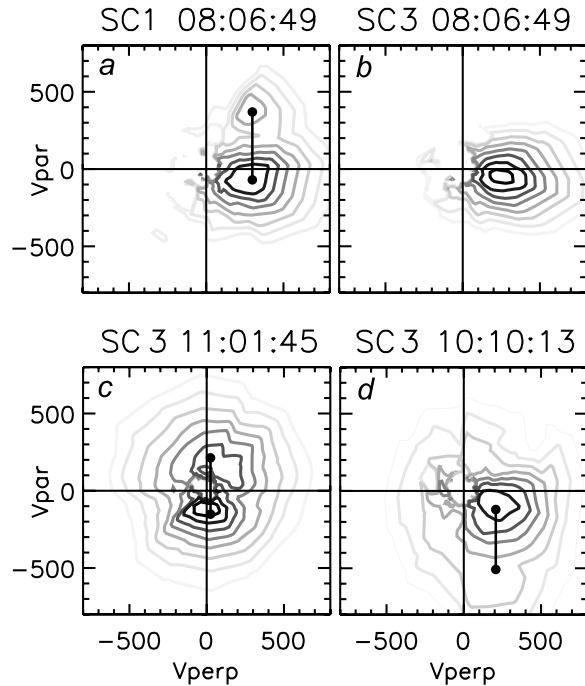


Figure 3. Four cuts of the ion distribution functions in the V_{\parallel} - V_{\perp} plane by HIA. (top) Two simultaneous measurements (a) by SC1 (in the MSBL) and (b) by SC3 (in the magnetosheath); (bottom) taken by SC3 in the MSBL (c) sunward of the reconnection site and (d) tailward of it. Of the two populations in the MSBL, the one with the larger phase space density is the incident magnetosheath population, and the other is the reflected magnetosheath population. The vertical segments between the two populations represent the expected separation ($2V_A$).

Figure 3d, the reflected population (indicated by the widely spaced contours) streams antiparallel to the convected magnetic field, so that now the spacecraft is tailward of the reconnection site (side C of Figure 1c). In both cases (Figures 3c and 3d) the two peaks are separated by $2V_A$, as indicated by the vertical bar drawn on each plot. Note that unless otherwise explicitly stated, for all the distribution functions presented in this paper, HIA data have been used because of their higher temporal resolution, but the examination of CODIF data (not shown) confirms that these ions are protons. There are also cases (Figures 4a and 4b) in which, within a short time interval, SC3 encounters the MSBL on opposite sides of the reconnection site. For example, at 1059:53 UT the spacecraft is sunward of the reconnection site, as the reflected ions flow parallel to the convected magnetic field, and at 1058:52 UT it is tailward of the reconnection site, as now the reflected ions (indicated by the widely spaced contours enclosed in the dashed box) flow antiparallel to the convected field. This indicates that the reconnection site passes over the spacecraft within a short time interval.

[6] Figures 4c and 4d are examples of BL observations. They show the transmitted magnetosheath populations that have the characteristic D shape: the first flows antiparallel to \mathbf{B} , and therefore the spacecraft is located sunward of the reconnection site (side B of Figure 1c), and the second, only

36 s earlier, is parallel to \mathbf{B} (i.e., spacecraft tailward of the reconnection site, side D of Figure 1c). The important point derived from the above examples is that SC3 is alternately located tailward or sunward of the reconnection site, both in the MSBL and in the BL. Examples such as those of Figure 4 are very frequent throughout the event, so that SC3 is always close to the reconnection site. SC1 and SC4 are, most of the time, sunward of the reconnection site, consistent with their position relative to SC3 and only rarely move tailward of the reconnection site. This suggests that the distance of SC3 from the reconnection site can be inferred using data from two spacecraft. A survey of the data allowed to select two overlapping observations, one by SC4 (1005:57 UT), and one by SC3 (1006:00 UT) (Figure 5), occurring on opposite sides of the reconnection site. SC4 (Figure 5a) is in the BL sunward of the reconnection site (side B of Figure 1c). SC3 (Figure 5b) is in the MSBL tailward of it (side C of Figure 1c) and detects incident and reflected magnetosheath ions: the latter (in the dashed box) are evidenced by the widely spaced contours antiparallel to the convected magnetic field. This means that the distance of the spacecraft from the reconnection site is surely smaller than the separation between SC3 and SC4 (Figure 1b), that is below 3200 km, in excellent agreement with the estimate of 2500 km obtained by *Retinò et al.* [2006] at 1058 UT, based on a comparison with numerical simulations.

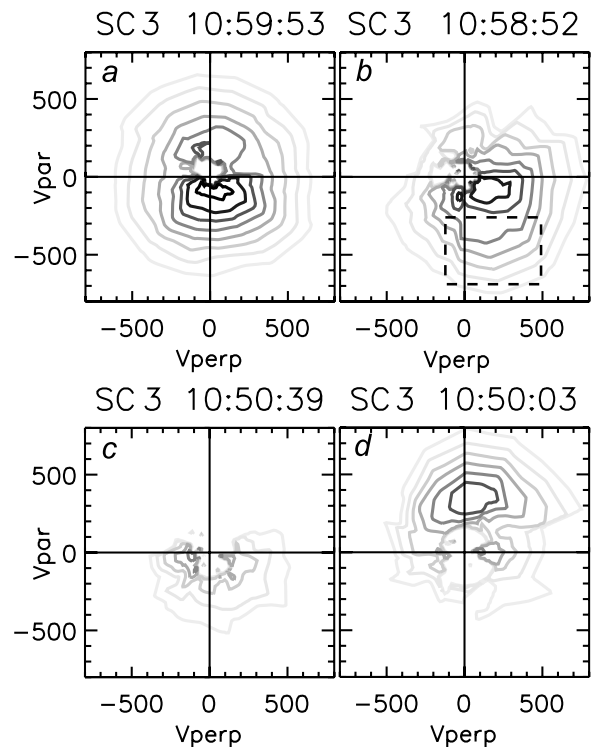


Figure 4. Same format as Figure 3. (top) SC3 is in the MSBL, (a) sunward and (b) tailward of the reconnection site. The incident and reflected magnetosheath ions are shown: in Figure 4a the reflected ions flow parallel to \mathbf{B} and in Figure 4b they flow antiparallel and are enclosed in the dashed box. (bottom) SC3 is in the BL (c) sunward and (d) tailward of the reconnection site.

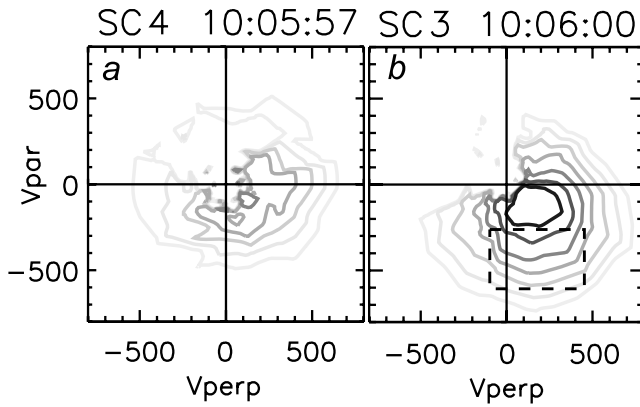


Figure 5. Same format as Figure 3. Two overlapping distribution functions (a) by CODIF for H^+ on SC4 and (b) by HIA on SC3. The former is in the BL sunward of the reconnection site and shows the transmitted magnetosheath ions and the latter is in the MSBL tailward of it. In Figure 5b, incident and reflected magnetosheath ions. The latter is enclosed in the dashed box.

[7] So far only protons have been considered. Between 0900 and 0945 UT SC3 is in the magnetosheath but has various partial encounters with the MP, entering only in the MSBL (and not in the BL) where it unambiguously detects O^+ ions. Figure 6 shows one example of O^+ observed by CODIF. At this time SC3 is in the MSBL sunward of the reconnection site: Figure 6a is the distribution function by HIA which shows the incident and reflected protons separated by $2V_A$ along the convected magnetic field. In Figure 6b are the simultaneous CODIF observations for O^+ (CODIF's time resolution for O^+ ions on SC3 is 32 s), which show O^+ traveling along the local convected magnetic field at a speed comparable to the reflected protons. O^+ ions are present in the nearby plasma mantle, as simultaneously observed by SC1 (not shown). Therefore these O^+ ions are transmitted magnetospheric ions propagating along the reconnected field lines. The observations are consistent with predictions [Fuselier, 1995] because transmitted ions, regardless of their mass, upon crossing the current sheet

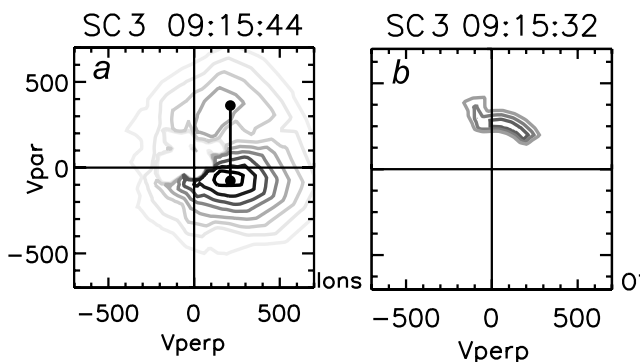


Figure 6. Same format as Figure 3. (a) Incident and reflected H^+ ions in the MSBL as seen by HIA on SC3 (the incident population has the larger phase space density). (b) Simultaneous measurement of O^+ (i.e., transmitted magnetospheric ions) by CODIF, also on SC3.

gain a velocity component along \mathbf{B} comparable to the reflected magnetosheath population.

4. Field Line Convection and Quantitative Comparison With Theoretical Expectations

[8] Reconnected field lines move with the de Hoffmann-Teller velocity (V_{HT}) in the spacecraft frame and, of course, different V_{HT} velocities are expected on the two sides of the reconnection site. Cooling *et al.* [2001] developed a numerical model to determine the motion of reconnected flux tubes, depending on the reconnection location for a given IMF orientation. As discussed in detail by Gosling *et al.* [1991], for the geometry of the present event, in the spacecraft frame, tailward of the reconnection site the field lines convect tailward with $V_{HT} > V_A$ [Cooling *et al.*, 2001], V_A being the magnetosheath Alfvén speed, and both the reflected and transmitted magnetosheath populations move tailward with a speed larger than the incident magnetosheath speed, V_{sh} . Sunward of the reconnection site, the cases of sub-Alfvénic and super-Alfvénic magnetosheath flow must be considered separately. In the former case ($M_A < 1$) the field lines contract sunward and the reflected and transmitted magnetosheath populations are directed sunward with a speed greater than V_{sh} . In the latter case ($1 < M_A < 2$) the field lines contract tailward, but the reflected and transmitted magnetosheath populations still move sunward with a speed smaller than V_{sh} . Therefore lobe reconnection induces sunward convection of the field lines only in the case of sub-Alfvénic magnetosheath flow.

[9] In order to obtain a good V_{HT} velocity, the discontinuity must be one-dimensional and time stationary. This is not always the case in the present event, because some of the MP crossings have a complicated structure, suggestive of nonmonotonic motion of the MP. Moreover, as shown in section 3, there are cases in which the spacecraft enters the current sheet in the MSBL tailward (sunward) of the reconnection site and exits in the BL sunward (tailward) of it, indicating that when crossing the MP, the spacecraft does not encounter the same field line in the MSBL and in the BL. For all of the above reasons one cannot expect to find a good dHT frame and the observations confirm that in many MP crossings a poor dHT frame is obtained. There are however a few cases in which the spacecraft crosses the MP either always tailward or always sunward of the reconnection site, and for these cases a good V_{HT} velocity can be determined: a few representative examples are listed in Table 1. One example of MP crossing tailward of the reconnection site is shown in Figure 7: here the magneto-

Table 1. Three Cases in Which a Good V_{HT} was Obtained^a

Time, UT	V_{HT}	V_{HT}	V_R	V_T	V_A	V_{sh}	M_A
1057:54–1058:50	–180 220 –120	309	300 T	500 T	217	158	0.7
1103:53–1105:26	110 –64 59	140	190 S	212 S	265	174	0.7
1013:18–1013:50	–11 –21 –60	64	180 S	160 S	153	190	1.2

^aFrom the left are shown the time interval, the components and magnitude of the measured V_{HT} ; V_R and V_T (i.e., the measured speed of the reflected and transmitted magnetosheath ions observed in the MSBL and in the BL, respectively), the Alfvén speed, the magnetosheath flow speed (all speeds in km/s), and the Alfvén Mach number. Labels T and S indicate tailward (i.e., antisunward-duskward-southward) and sunward (i.e., sunward-dawnward-northward) flows, respectively.

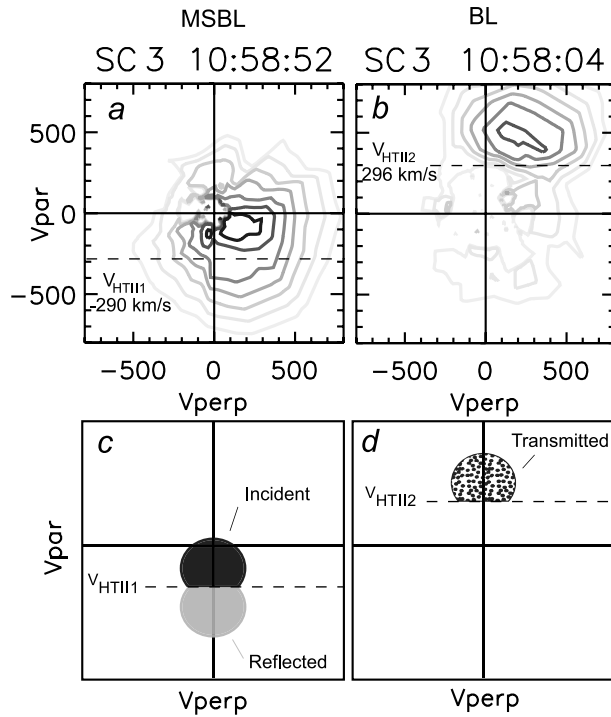
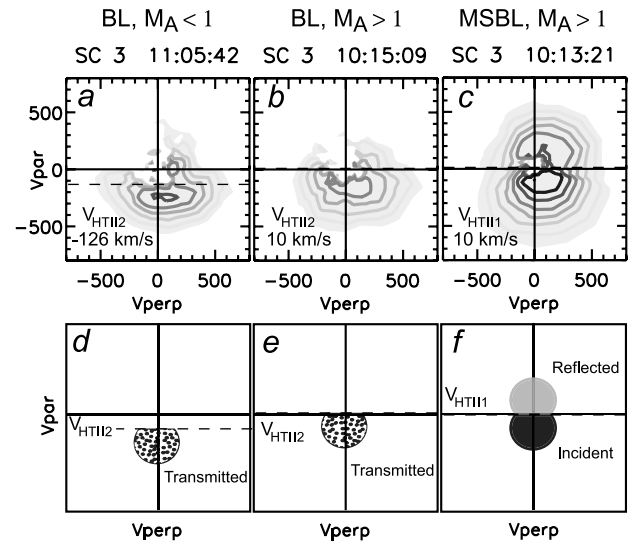


Figure 7. (top) Same format as Figure 3. Two distribution functions (a) in the MSBL and (b) in the BL, tailward of the reconnection site for the first crossing of Table 1. The distribution function in Figure 7a is the same as in Figure 4b: it represents the incident and reflected ions in the MSBL. In Figures 7a and 7b the horizontal dashed lines are at $V_{\text{HT||1}}$ and $V_{\text{HT||2}}$, respectively; that is, they are the components of the measured V_{HT} along \mathbf{B} in the MSBL and in the BL. (bottom) Corresponding sketches (adapted from Cowley [1995]) that indicate the expected position in the V_{\parallel} - V_{\perp} plane (c) of the incident and reflected magnetosheath ions in the MSBL and (d) of the transmitted magnetosheath ions in the BL, as seen by an observer tailward of the reconnection site. Note that for simplicity, in Figures 7c and 7d the convection velocity has been neglected.

sheath speed is sub-Alfvénic ($M_A = 0.7$) and the magnetic shear angle at the MP is high (176°). M_A is measured in the magnetosheath proper, close to the MSBL. Table 1 shows that V_{HT} is directed tailward and is larger than V_A , as expected for observations tailward of the reconnection site. Figures 7c and 7d (adapted from Cowley [1995]) show the expected location, in the V_{\parallel} - V_{\perp} plane, of the various populations in the MSBL and in the BL, respectively. Note that tailward flows have $V_{\parallel} < 0$ in the magnetosheath and $V_{\parallel} > 0$ in the BL. The sketches show that only the part of the incident distribution function which has, in the dHT frame, $V_{\parallel}^{\text{HT}} > 0$ ($V_{\parallel}^{\text{HT}}$ is the velocity in the dHT frame), (i.e., $V_{\parallel} > V_{\text{HT||1}}$ in the spacecraft frame) will be transmitted through the MP. Subscripts 1 and 2 indicate the $V_{\text{HT||}}$ component parallel to the MSBL and BL fields, respectively. Figures 7a and 7b are observations in the MSBL and in the BL, respectively: in the MSBL the incident and reflected populations are shown, the latter appearing as a deformation in the contours. In Figure 7a the dashed line at $V_{\parallel} = V_{\text{HT||1}}$, obtained from the measured V_{HT} , is very close

to the separation between the incident (with $V_{\parallel} > V_{\text{HT||1}}$) and the reflected population, and in the BL (Figure 7b) the line at $V_{\parallel} = V_{\text{HT||2}}$ is in excellent agreement with the low-energy cutoff of the D-shaped transmitted magnetosheath distribution. Table 1 shows also that in the spacecraft frame, V_R and V_T are both directed tailward and are greater than V_{sh} , as expected. At the 1104 UT crossing listed in Table 1, M_A is 0.7, SC3 is sunward of the reconnection site, and the shear angle is high (166°). The distribution function in the BL is shown in Figure 8a, and the corresponding predictions are shown in Figure 8d. Now the part of the magnetosheath distribution function which is transmitted across the MP has $V_{\parallel}^{\text{HT}} < 0$ in the V_{HT} frame, i.e., $V_{\parallel} < V_{\text{HT||1}}$, namely flows antisunward in the MSBL (not shown) and sunward in the BL (Figures 8a and 8d). Table 1 shows that as expected, V_{HT} is directed sunward and the dashed line in Figure 8a is again comparable with the low-energy cutoff of the D-shaped distribution function. From Table 1 it is seen that V_R and V_T are also directed sunward with a speed larger than V_{sh} , as expected.

[10] Another crossing sunward of the reconnection site occurs at 1013 UT (Figures 8b and 8c): the shear angle is again high (162°), but now $M_A = 1.2$. In this case the field line convection speed, V_{HT} , is expected to be small and tailward [Gosling *et al.*, 1991]. Table 1 confirms that V_{HT} , predominantly tailward, is much smaller than in the previous case (64 km/s), and that V_R , V_T are directed sunward and are smaller than V_{sh} . In Figures 8b and 8c the distribution



Sunward case

Figure 8. (top) Same format as Figure 3. (a, b, c) Observed sunward of the reconnection site: Figure 8a is in the BL for $M_A < 1$, Figures 8b and 8c are in the BL and in the MSBL, respectively, for $M_A > 1$. (d, e, f) Corresponding sketches similar to the ones of Figure 7 but for an observer sunward of the reconnection site: Figure 8d shows the predicted transmitted magnetosheath ions in the BL, for $M_A < 1$. Figures 8e and 8f show the expected distribution function in the BL and in the MSBL, respectively, for $M_A \geq 1$.

functions in the BL and in the MSBL are shown, and in Figures 8e and 8f are the corresponding predicted distribution functions. The low-energy cutoff of the D-shaped distribution function in the BL (Figure 8b) is very close to the predicted value indicated by the dashed line, and also the separation between the incident and reflected magnetosheath population in the MSBL (Figure 8c) agrees with the expected value indicated by the dashed line.

5. MP Crossing at 1135 UT and Evidence of Dual Reconnection

[11] The MP inbound crossing at 1135 UT will be now described in detail, because it has some interesting peculiarities. Figure 9 (top) is the time history of this crossing. Initially, SC3 is in the magnetosheath, characterized by a large negative B_Y component. Then, at around 1133:30 UT, there is a partial MP crossing (evidenced by the brief change in B_Z) and later the complete field rotation takes place between 1134:15 and 1137:15 UT. At the end of the interval SC3 is in the BL. The magnetosheath flow is sub-Alfvénic with $M_A = 0.6$.

[12] The distribution functions at the times indicated by the dashed lines are plotted in the $V_{\parallel} - V_{\perp}$ plane. During the partial brief encounter with the MSBL at 1133:30 UT, the distribution function (Figure 9a) is typical of the MSBL sunward of the reconnection site. After briefly returning to the magnetosheath proper, SC3 reenters the MSBL (Figure 9b) for the complete MP crossing. Now three populations are present: the one with the largest phase space density (i.e., at small energy, antiparallel to \mathbf{B}) is the incident magnetosheath population, and the other two are secondary populations. All three have an anisotropy $T_{\perp} > T_{\parallel}$. The corresponding Figure 9d shows a double-humped profile antiparallel to \mathbf{B} and one peak parallel to \mathbf{B} . The similarity between the two secondary populations suggests a common magnetosheath origin. Of the two secondary populations, the one which streams parallel to \mathbf{B} is similar to the reflected population sunward of the reconnection site, and the other to the reflected population tailward of the reconnection site (e.g., Figure 4b). Therefore the two secondary populations could at first sight be interpreted as the effect of the motion of the reconnection site relative to the spacecraft during the sampling time. However, this hypothesis must be ruled out because the three populations are present in eight consecutive spectra. Moreover the separation between the main population and the parallel one is not too far from $2V_A$ (indicated by the horizontal bar), whereas the separation between the two populations antiparallel to \mathbf{B} is much smaller. This indicates that the main population and the parallel population are the incident and reflected magnetosheath populations, respectively, seen by an observer sunward of the reconnection site.

[13] Regarding the third population, one possible interpretation suggests a non local origin, namely the existence of a second reconnection site in the northern hemisphere. The open end of the southern hemisphere MSBL field line, sunward of the reconnection site, after having been convected sunward around the dayside MP while it is diverted tailward-northward-downward, could re-reconnect in the northern dawn hemisphere with the local lobe field lines, generating a newly closed reconnected field line in addition

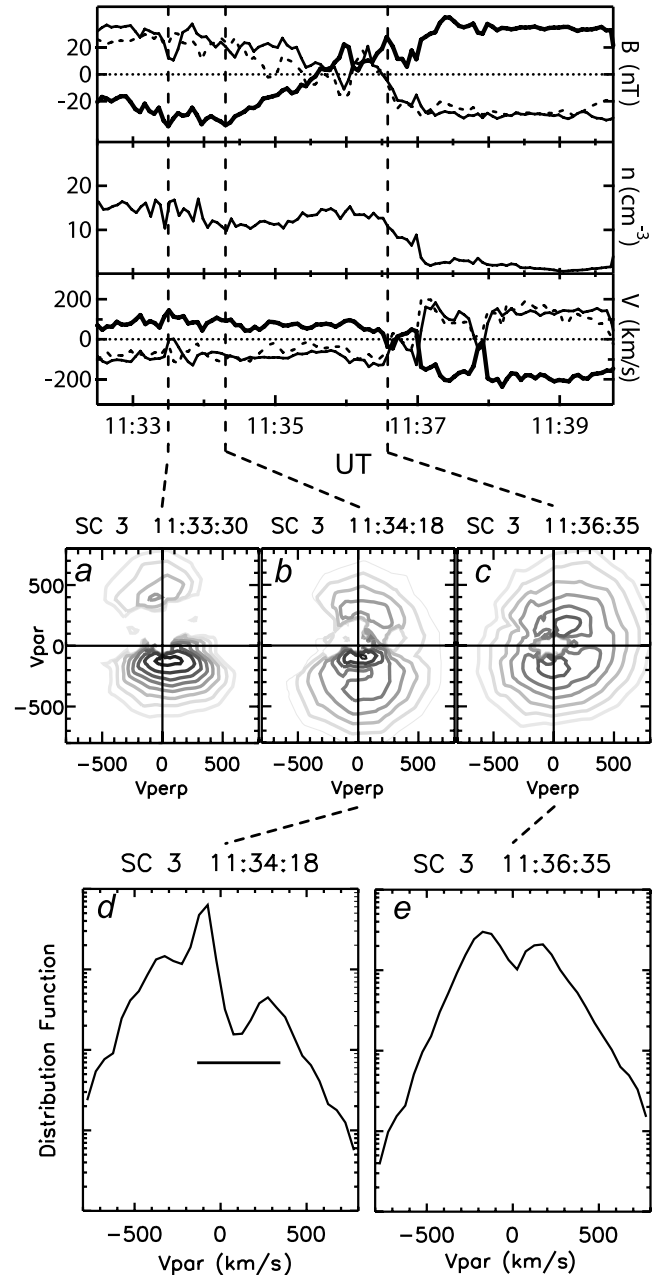


Figure 9. (top) Time history of the 1134–1136 UT MP crossing by SC3. In the B and V plots the dashed line the x component and the thick line the y component. (middle) Same format as Figure 3. Observations in the MSBL (Figures 9a and 9b) and in the BL (Figure 9c) at the times indicated by the dashed lines. (a) A typical MSBL observation sunward of the reconnection site, (b) still in the MSBL but with three field-aligned populations (the main population is at low energy and flows antiparallel to \mathbf{B} and the two secondary populations flow in opposite directions along \mathbf{B}). (c) Two counterstreaming populations in the BL. (d and e) Profiles along V_{\parallel} of the distribution functions of Figures 9b and 9c, respectively. The horizontal bar in Figure 9d indicates the $2V_A$ separation between incident and locally reflected ions.

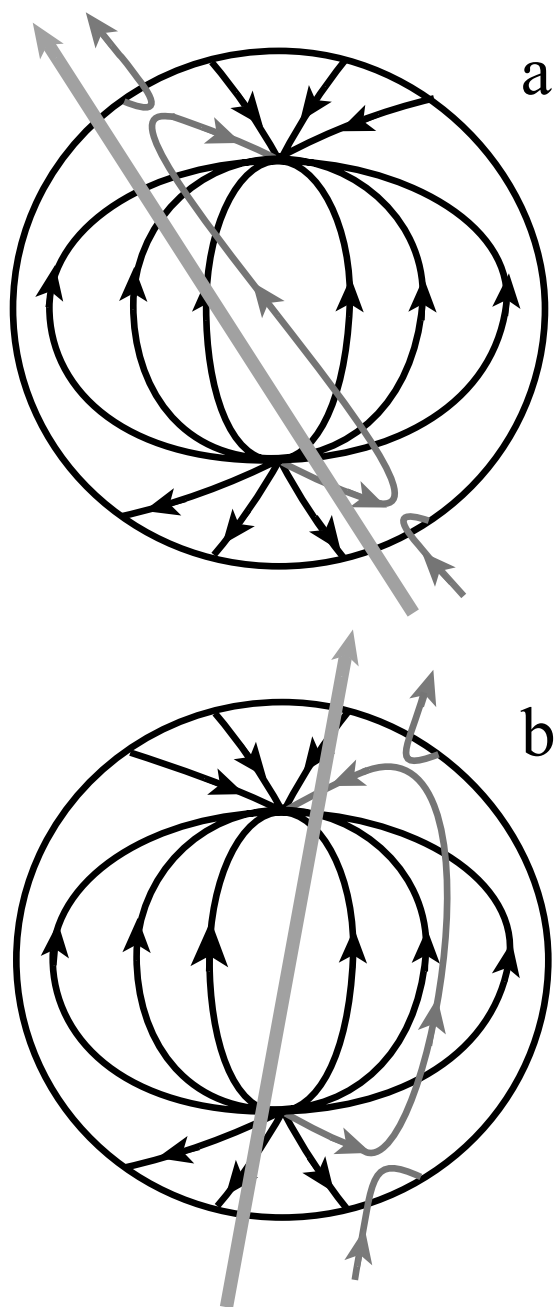


Figure 10. Sketches of the dual lobe reconnection topology in the case of (a) $B_Y < 0$ and (b) $B_Y > 0$ in the magnetosheath (view from the Sun). The grey straight line is the IMF and the other grey lines are the newly reconnected field lines.

to a fully detached field line. In this hypothesis the MSBL would be a closed field line connecting the two reconnection sites in opposite hemispheres. A sketch of this configuration is represented in Figure 10a.

[14] At the northern dawn quadrant, at the location of this hypothetical second reconnection site, the incident magnetosheath flow is draped around the magnetopause and therefore is roughly parallel to the magnetosheath magnetic field. The newly closed field line would contract equatorward, that is the local V_{HT} would be opposite to the

magnetosheath flow, and a hypothetical magnetosheath population reflected at that reconnection site would propagate antiparallel to \mathbf{B} . This is exactly what the observations of Figure 9b shows, namely the spacecraft is in the MSBL sunward of the reconnection site in the southern hemisphere and observes, besides the local incident and reflected magnetosheath ions, a higher energy population which consists of magnetosheath ions reflected at a second reconnection site in the northern dawn hemisphere propagating southward antiparallel to \mathbf{B} . Note that as reconnection is going on for a long time during this event, 1 keV particles starting from the opposite hemisphere have plenty of time to reach Cluster. Later on, in the outer BL, at 1136:35 UT (Figure 9c and profile in Figure 9e) the distribution function consists of two symmetrical counterstreaming distribution functions: at low energies the one antiparallel to \mathbf{B} has a slightly larger phase space density and the other is somewhat heated, but above 500 km/s the two profiles are almost identical. The former is the transmitted magnetosheath population, and the latter we interpret as the same population which has travelled to the ionosphere, has mirrored at low altitude and has returned to the spacecraft. Note that the absence of a low-energy cutoff in the mirrored population is a consequence of the long duration of the present reconnection event, which makes all time of flight effects negligible.

[15] Finally SC3 enters in the BL: between 1137:07 and 1139:48 UT, in the inner BL, the transmitted magnetosheath distribution functions are almost all D-shaped (not shown) flowing antiparallel to \mathbf{B} , as expected for observations sunward of the reconnection site. The corresponding sunward speed, as shown in the time history of Figure 9, is much larger than the magnetosheath speed ($V_{BL} = 270$ km/s, $V_{sh} = 150$ km/s), consistently with the low Alfvén Mach number of the magnetosheath flow.

6. Discussion

6.1. Kinetic Aspects

[16] A remarkable characteristic of the present event is the large number of kinetic signatures related to reconnection: almost all encounters with the MP by the three Cluster spacecraft have secondary populations. At inbound crossings, in almost all MSBL passes, as soon as \mathbf{B} starts to rotate, secondary populations appear (usually reflected magnetosheath protons and in a few cases transmitted magnetospheric O^+ ions). Similarly, almost all the BL encounters have reconnection flows, often D-shaped, for the majority of which the Walén test was successfully verified by *Retinò et al.* [2005]. Predictions by kinematic considerations [Cowley, 1982, 1995] allow characterizing the distribution functions across the MP both sunward and tailward of the reconnection site. Therefore the detailed inspection of the distribution functions in the MSBL and in the BL allows inferring that the reconnection site very frequently moves even on short timescales, so that SC3 is alternately located sunward or tailward of the reconnection site. However, the important result is that the displacements of the reconnection site are small, so that often, throughout the event, SC3 is close to the reconnection site (< 3200 km). This extends the previous finding of *Retinò et al.* [2005], who infer the vicinity to the reconnection site for the time interval where flow reversals are observed in the BL. One of

these flow reversal intervals which occur for low magnetic shear angle, allowed *Retinò et al.* [2005] to infer that component merging was going on at that time. The present study evidences that SC3 is often close to the reconnection site also in the earlier part of the event, when the local magnetic shear is low. This indicates the occurrence of component merging also in other intervals. In the case of the incident/reflected populations in the MSBL, the predictions are that the separation between the peaks be $2V_A$; this check has been done in many cases and usually gives good agreement, both sunward and tailward of the reconnection site. In the case of the transmitted magnetosheath ions, a quantitative comparison of the D-shaped cutoff with predictions needs the determination of a reliable V_{HT} , which is not always possible because of the nonstationarity of most MP crossings. However, in the few cases in which a good V_{HT} could be obtained, a satisfactory agreement with predictions was found, regarding both the distribution functions and the field line convection.

[17] Although kinetic signatures related to reconnection have been repeatedly reported in the literature [e.g., *Gosling et al.*, 1991, 1996; *Fuselier*, 1995; *Fuselier et al.*, 1995, 1997; *Bauer et al.*, 2001; *Vaisberg et al.*, 2004], they are not present at all the MP crossings which satisfy the Walén test. For instance, *Bauer et al.* [2001], in a statistical study, report that they observe D-shaped distribution functions in the transmitted magnetosheath and magnetospheric populations “only for the minority of the Walén events.” Also *Phan et al.* [2004] say that even in clear reconnection events, the transmitted magnetosheath population in the BL does not always display the characteristic D shape and suggest that one reason could be the distance from the reconnection site. The reason why D-shaped distributions are observed in some reconnection events and not in others is to date not understood [*Phan et al.*, 2005]. The present study seems to confirm the crucial role of the distance from the X line. Indeed in this event Cluster is almost always close to the reconnection site and detects reflected magnetosheath ions in almost all the MSBL encounters and D-shaped distribution functions in many of the BL encounters.

[18] One interesting point emerges from the inspection of the entire event: it is seen that throughout the event, sunward transmitted magnetosheath flows usually occur earthward of the field rotation (see, e.g., the one occurring after 1137 UT in the time history of Figure 9), whereas tailward transmitted magnetosheath flows usually occur during the magnetic field rotation. A clear example of this is shown in Figure 3 of *Retinò et al.* [2005], where tailward reconnection flows 1 and 4 occur during the field rotation, while sunward reconnection flows 2 and 3 occur earthward of the field rotation. This observational fact is consistent with the simulations performed by *La Belle-Hamer et al.* [1995], which predict separate locations within the current sheet for transmitted magnetosheath ions tailward and sunward of the reconnection site in the case of MP crossings with velocity shear (as is the case in the flanks or at high latitude). The predictions are that when the spacecraft is tailward of the reconnection site “the accelerated flow is confined to the field reversal region,” whereas when the spacecraft is sunward of the reconnection site, “the accelerated flow is on the magnetospheric side of the field

reversal region.” This is exactly what Cluster sees during the present event.

6.2. Global Configuration of the Merging Process

[19] Reconnection takes place close to the spacecraft in the southern hemisphere, which is favored both because the observations occur at the winter solstice and also because the magnetosheath magnetic field has a positive B_X [*Crooker*, 1992; *Fuselier et al.*, 1997]. However, in section 5 the observations of three simultaneous populations in the MSBL allowed us to infer that at least during a limited time, dual reconnection was going on. The presence of three populations in the MSBL is not limited to that unique case, but occurs in a few other cases (not shown) at around 0930 UT. Here again the incident and locally reflected populations are separated by $\sim 2V_A$, and the anti-parallel population originates in the northern hemisphere. The only difference with respect to the case discussed in section 5 is that now the magnetosheath B_Y is slightly positive (see section 2), so that the second reconnection site is in the northern dusk quadrant: the corresponding sketch is shown in Figure 10b. The existence of a second reconnection site has important implications for the topology of the reconnection process and for the dynamics of the magnetosphere. In principle the second reconnection site could be either tailward or equatorward of the cusp, and it is not possible, from this kind of measurements in the southern hemisphere, to distinguish between the two possibilities; however, the local shear is expected to be higher tailward than equatorward of the cusp, so that the former should be favored. A confirmation of dual lobe reconnection for this event has been recently obtained by *Marcucci et al.* [manuscript in preparation] through the analysis of SuperDARN and IMAGE FUV data for the northern hemisphere. Dual lobe reconnection for strongly northward IMF was initially proposed by *Song and Russell* [1992] as a mechanism for the formation of the low-latitude boundary layer and observational evidence was later obtained by *Onsager et al.* [2001] in a lobe reconnection event at 12 LT occurring for northward IMF.

7. Conclusions

[20] The analysis of the 3 December 2001 lobe reconnection event suggests the following scenario:

[21] 1. IMF is northward with variable B_Y and Cluster observes lobe reconnection quasi-continuously over four hours in the southern dusk high-latitude hemisphere, as confirmed by the large number of secondary populations related to reconnection, present at most of the MP encounters.

[22] 2. The reconnection site moves frequently across SC3; however, simultaneous multipoint observations allow us to infer that the spatial scale of this displacement is small, so that the spacecraft is always close to the reconnection site (< 3200 km). Moreover, the vicinity to the reconnection site over an extended time is probably the cause of the presence of a large number of secondary populations related to reconnection and of the fact that the detailed characteristics of the distribution functions within the current layer, as well as the reconnected field lines motion, agree with theoretical predictions.

[23] 3. The magnetosheath flow is sub-Alfvénic in the vicinity of the X line, consistent with the long duration of this reconnection event.

[24] 4. Reconnection is observed in situ in the southern hemisphere and, during a few limited time intervals, there is observational evidence that it is also simultaneously active in the northern hemisphere.

[25] **Acknowledgments.** The work done at IFSI has been supported by the Agenzia Spaziale Italiana under contract I/035/05/0 ASI/INAF-OATO. A. Retinò is supported by the Swedish National Space Board. The authors thank one of the referees for constructive comments.

[26] Amitava Bhattacharjee thanks Steven Petrinec and Xiaogang Wang for their assistance in evaluating this paper.

References

- Avanov, L. A., V. N. Smirnov, J. H. Waite Jr., S. A. Fuselier, and O. L. Vaisberg (2001), High-latitude magnetic reconnection in sub-Alfvénic flow: Interball Tail observations on May 29, 1996, *J. Geophys. Res.*, *106*, 29,491–29,502.
- Balogh, A., et al. (2001), The Cluster Magnetic Field Investigation: Overview of in-flight performance and initial results, *Ann. Geophys.*, *19*, 1207–1217.
- Bauer, T. M., G. Paschmann, N. Sckopke, R. A. Treumann, W. Baumjohann, and T.-D. Phan (2001), Fluid and particle signatures of dayside reconnection, *Ann. Geophys.*, *19*, 1045–1063.
- Cooling, B. M. A., C. J. Owen, and S. J. Schwartz (2001), Role of the magnetosheath flow in determining the motion of open flux tubes, *J. Geophys. Res.*, *106*, 18,763–18,775.
- Cowley, S. W. H. (1982), The causes of convection in the Earth's magnetosphere: A review of developments during the IMS, *Rev. Geophys.*, *20*, 531–565.
- Cowley, S. W. H. (1995), Theoretical perspectives of the magnetopause: A tutorial review, in *Physics of the Magnetopause*, *Geophys. Monogr. Ser.*, vol. 90, edited by P. Song, B. U. O. Sonnerup, and M. F. Thomsen, pp. 29–44, AGU, Washington, D. C.
- Crooker, N. U. (1992), Reverse convection, *J. Geophys. Res.*, *97*, 19,363–19,372.
- Fuselier, S. A. (1995), Kinetic aspects of reconnection at the magnetopause, in *Physics of the Magnetopause*, *Geophys. Monogr. Ser.*, vol. 90, edited by P. Song, B. U. O. Sonnerup, and M. F. Thomsen, pp. 181–187, AGU, Washington, D. C.
- Fuselier, S. A., B. J. Anderson, and T. G. Onsager (1995), Particle signatures of magnetic topology at the magnetopause: AMPTE/CCE observations, *J. Geophys. Res.*, *100*, 11,805–11,821.
- Fuselier, S. A., B. J. Anderson, and T. G. Onsager (1997), Electron and ion signatures of field line topology at the low-shear magnetopause, *J. Geophys. Res.*, *102*, 4847–4863.
- Gosling, J. T., et al. (1982), Evidence for quasi-stationary reconnection at the dayside magnetopause, *J. Geophys. Res.*, *87*, 2147–2158.
- Gosling, J. T., M. F. Thomsen, S. J. Bame, R. C. Elphic, and C. T. Russell (1991), Observations of reconnection of interplanetary and lobe magnetic field lines at the high-latitude magnetopause, *J. Geophys. Res.*, *96*, 14,097–14,106.
- Gosling, J. T., M. F. Thomsen, G. Le, and C. T. Russell (1996), Observations of magnetic reconnection at the lobe magnetopause, *J. Geophys. Res.*, *101*, 24,765–24,774.
- Kessel, R. L., S.-H. Chen, J. L. Green, S. F. Fung, S. A. Boardsen, L. C. Tan, T. E. Eastman, J. D. Craven, and L. A. Frank (1996), Evidence of high-latitude reconnection during northward IMF: Hawkeye observations, *Geophys. Res. Lett.*, *23*, 583–586.
- La Belle-Hamer, A. L., A. Otto, and L. C. Lee (1995), Magnetic reconnection in the presence of sheared flow and density asymmetry: Applications to the Earth's magnetopause, *J. Geophys. Res.*, *100*, 11,875–11,890.
- Marcucci, M. F., et al. (2000), Evidence for interplanetary magnetic field B_Y controlled large-scale reconnection at the dayside magnetopause, *J. Geophys. Res.*, *105*, 27,497–27,508.
- Onsager, T. G., J. D. Scudder, M. Lockwood, and C. T. Russell (2001), Reconnection at the high-latitude magnetopause during northward interplanetary magnetic field conditions, *J. Geophys. Res.*, *106*, 25,467–25,488.
- Phan, T. D., et al. (2000), Extended magnetic reconnection at the Earth's magnetopause from detection of bi-directional jets, *Nature*, *404*, 848–850.
- Phan, T.-D., et al. (2003), Simultaneous Cluster and IMAGE observations of cusp reconnection and auroral proton spot for northward IMF, *Geophys. Res. Lett.*, *30*(10), 1509, doi:10.1029/2003GL016885.
- Phan, T. D., et al. (2004), Cluster observations of continuous reconnection at the magnetopause under steady interplanetary magnetic field conditions, *Ann. Geophys.*, *22*, 2355–2367.
- Phan, T.-D., C. P. Escoubet, L. Rezeau, R. A. Treumann, A. Vaivads, G. Paschmann, S. A. Fuselier, D. Attié, B. Rogers, and B. U. Ö. Sonnerup (2005), Magnetopause processes, in *Outer Magnetospheric Boundaries: Cluster Results*, *Space Sci. Ser.*, vol. 20, edited by G. Paschmann et al., pp. 367–424, Springer, New York.
- Rème, H., et al. (2001), First multispacecraft ion measurements in and near the Earth's magnetosphere with the identical Cluster ion spectrometry (CIS) experiment, *Ann. Geophys.*, *19*, 1303–1354.
- Retinò, A., et al. (2005), Cluster multispacecraft observations at the high-latitude duskside magnetopause: Implications for continuous and component magnetic reconnection, *Ann. Geophys.*, *23*, 461–473.
- Retinò, A., et al. (2006), Structure of the separatrix region close to a magnetic reconnection X-line: Cluster observations, *Geophys. Res. Lett.*, *33*, L06101, doi:10.1029/2005GL024650.
- Safrankova, J., Z. Nemecek, D. G. Sibeck, L. Prech, J. Merka, and O. Santolik (1998), Two-point observation of high-latitude reconnection, *Geophys. Res. Lett.*, *25*, 4301–4304.
- Song, P., and C. T. Russell (1992), Model of the formation of the low-latitude boundary layer for strongly northward interplanetary magnetic field, *J. Geophys. Res.*, *97*, 1411–1420.
- Vaisberg, O. L., L. A. Avanov, T. E. Moore, and V. N. Smirnov (2004), Ion velocity distributions within the LBL and their possible implication to multiple reconnections, *Ann. Geophys.*, *22*, 213–236.
- A. Balogh, Space and Atmospheric Physics, Blackett Laboratory, Imperial College, Prince Consort Road, London SW7 2BZ, UK.
- M. B. Bavassano Cattaneo, M. F. Marcucci, and G. Pallochia, Istituto di Fisica dello Spazio Interplanetario, INAF, Area della Ricerca di Tor Vergata, Via del Fosso del Cavaliere 100, I-00133 Rome, Italy. (maria.bice.cattaneo@ifsi-roma.inaf.it)
- C. W. Carlson, Space Sciences Laboratory, University of California, 7 Gauss Way, Berkeley, CA 94720-7450, USA.
- I. Dandouras and H. Rème, Centre d'Etude Spatiale des Rayonnements, 9 Avenue du Colonel Roche, B.P. 4346, F-31028 Toulouse Cedex 4, France.
- L. M. Kistler, Space Science Center, Center for Earth, Oceans and Space, University of New Hampshire, Durham, NH 03824, USA.
- B. Klecker, Max-Planck-Institut für Extraterrestrische Physik, Karl-Schwarzschild Str. 1, Postfach 1312, D-85741 Garching, Germany.
- A. Korth, Max-Planck-Institut für Sonnensystemforschung, Max-Planck-Str. 2, D-37191 Katlenburg-Lindau, Germany.
- R. Lundin, Swedish Institute of Space Physics, P.O. Box 812, SE-981 28 Kiruna, Sweden.
- M. McCarthy, Geophysics Program, University of Washington, ATG Bldg., Box 351650, Room 202, Seattle, WA 98195-1650, USA.
- A. Retinò, Swedish Institute of Space Physics, Box 537, Uppsala, SE-75121 Sweden.